Interfacial coupling and its size dependence in $PbTiO_3$ and $PbMg_{1/3}Nb_{2/3}O_3$ multilayers

R. Ranjith,[1,*] R. Nikhil,[2] and S. B. Krupanidhi[1,*]
[1]*Materials Research Centre, Indian Institute of Science, Bangalore-12, India*
[2]*Department of Metallurgical and Materials Engineering, Indian Institute of Technology, Chennai-25, India*
(Received 1 June 2006; revised manuscript received 10 September 2006; published 6 November 2006)

Multilayers of $Pb(Mg_{1/3}Nb_{2/3})O_3$ (PMN)-$PbTiO_3$ (PT) were deposited through pulsed laser ablation deposition with different periodicities (d=10, 20, 30, 40, 50, 60, and 70 nm) for a constant total thickness of the film. The presence of superlattice reflections in the x-ray diffraction pattern clearly showed the superlattice behavior of the fabricated structures over a periodicity range of 20–50 nm. Polarization hysteresis and the capacitance-voltage characteristics of these films show clear size dependent ferroelectric and antiferroelectric (AFE) characteristics. Presence of long-range coupling and strain in multilayers with lower periodicity (~10 nm) exhibited a clear ferroelectric behavior similar to a solid solution of PMN and PT. Multilayers with higher periodicities (20–50 nm) exhibited antiferroelectric behavior, which could be understood from the energy arguments. On further increase of periodicity, they again exhibit ferroelectric behavior. The polarization studies were carried out beyond the Curie temperature T_c of PMN to understand the interlayer interaction. The interaction is changed to a ferroelectric-paraelectric interlayer and tends to lose its antiferroelectric behavior. The behavior of remnant polarization P_r and dP_r/dT with temperature clearly proves that the AFE coupling of these superlattices is due to the extrinsic interfacial coupling and not an intrinsic interaction as in a homogeneous conventional AFE material. The evidence of an averaged behavior at a periodicity of ~10 nm, and the behavior of individual materials at larger periodicities were further confirmed through dielectric phase transition studies. The presence of AFE interfacial coupling was insignificant over the dielectric phase transition of the multilayers.

DOI: 10.1103/PhysRevB.74.184104 PACS number(s): 77.80.Dj, 77.55.+f

I. INTRODUCTION

Fabrication and stabilization of materials that do not occur naturally has been the interest of study in recent trends of materials research.[1] Artificial superlattices (SL) and multilayers (ML) provide an opportunity to fabricate materials with carefully engineered properties. The control of desired properties can be achieved by tailoring the lattices.[2] The wide range of applications of ferroelectric oxides–ferroelectric memories, MEMS application, to name a few, require a precise combination of properties of individual layers. The materials used to form the SL may not have the required property individually.[3] Averaged physical behavior of the superlattice depends mainly upon the interfacial coupling among the layers and size of the individual layers. For example, neither $BaCuO_2$ nor $SrCuO_2$ is superconducting, but a superlattice of these materials exhibits superconductivity.[4] Thus, a better understanding of the coupling between the layers of the superlattice will help us understand the properties of the total combination, and is also crucial if we hope to synthesize superlattices with a particular property.[5] A ferroelectric (FE) SL cannot be assumed as a capacitor connected in a series, which would be an erroneous oversimplification of the problem. Various theoretical models explaining the role of the intrinsic coupling, the interfacial coupling, and the interfacial strain present in a ML has been studied extensively.[6–11] Theoretical studies of these SL and FE bilayers can be broadly classified into two major classes: the first one is based on a transverse Ising model (TIM), in which a model Hamiltonian is constructed including the interfacial exchange coupling among the ferroelectric (FE) dipoles of the different materials comprising the SL and their intrinsic dipolar coupling;[6,7,12,13] the second method is basically a continuum limit of the above explained discrete models,[7,14] in which the Landau free energy expression based on the polarization of the materials is constructed including the interfacial interaction among the polarization of the individual layers comprising the SL. The nature of the coupling is understood based on the energy arguments.[15]

Influence of the intrinsic and the interfacial coupling and their size dependences in a SL is well understood based on the TIM. The existence of the strong long-range FE interactions and their influence over the averaged property of a SL is studied on a FE-FE SL and also over a FE-paraelectric (PE) SL.[16,17] Existence of a strong long-range interaction across the interface and its dominance gives rise to a strong coupling within the layers, effectively giving an averaged property for the SL structure. A weak long-range interaction gives rise to the domination of interfacial coupling and hence the physical property due to the interfacial coupling between the layers is observed.[11] Most of the Ising models proposed were used to study the FE phase transition behavior, which is insensitive to the nature of either FE or AFE interfacial coupling.[6,7,12,18] Very few reports are found on the polarization hysteresis of the bilayers and multilayers (ML) based on these discrete models.[19] The effects of interfacial coupling giving rise to FE and AFE effects in a ML structure were explained based on the polarization behavior of the individual systems comprising the ML and energy considerations.[19] Interfacial coupling among the ferroelectric layers has also been studied based on the Landau free energy expression of the individual layers and a coupling term between the layers, which is a continuum model. These free energy constructions illustrate the role of interfacial coupling over the polarization behavior of the superlattices, and the existence of double loop behavior due to the AFE interfacial interaction among the layers present in the ferroelectric heterostructures and their dimensional dependent behavior.[15]

Experimentally, the existence of an intrinsic dipolar long-range interaction giving rise to an averaged FE behavior on epitaxial thin films has been observed in $KTaO_3/KNbO_3$ and in a relaxor superlattice.[20–22] For example, in the case of KTO/KNO SL, though one of the layers is a PE material at room temperature, the strain effects at the interface introduce a FE distortion and hence an effective FE behavior has been observed at low modulation lengths.[11,20] Evidence of an intrinsic coupling and an averaged behavior has also been observed in a FE relaxor SL;[22] whereas, an intrinsic size dependent FE and AFE distortion has been reported only on $SrTiO_3/BaZrO_3$ (STO/BZO) SL structure, in which the individual layers are room temperature PE in nature. A clear size dependent FE and AFE distortion has been observed in STO/BZO and KTO/KNO SL.[23,24] Knowledge of the interfacial interaction and its influence over the FE and AFE behavior of various ferroelectric heterostructures remains ambiguous. Moreover, an interaction between a normal FE and a relaxor FE ML has not been studied extensively. In the case of the FE heterostructures, certain questions remain ambiguous, for example what is the dimensional range in which the interfacial coupling dominates the overall polarization behavior of the system? Is it possible to observe the FE and AFE distortion in a ML structure of a normal FE and relaxor FE? Are the physical properties based on the individual layer dimensions tunable even in highly oriented polycrystalline structures, which are easier to fabricate in a mass scale and economic? In the present work, we have tried to address the above issues with lead magnesium niobate ($PbMg_{2/3}Nb_{1/3}O_3$) PMN, a well-known relaxor FE,[25–27] and lead titanate ($PbTiO_3$) PT, a well-known FE material.[28] Multilayers of PMN and PT were fabricated with different periodicities to study the interfacial coupling between the layers of the heterostructure. PMN is the most extensively studied relaxor with very high dielectric constant. PMN has a T_m (temperature corresponding to dielectric maxima) of ~ -15 °C. PMN also exhibits a frequency dependent T_m, which is a common phenomena observed in any of the relaxor FE. Above T_m, the PMN is known to behave as a superparaelectric system with nonzero remnant polarization (P_r).[25–27] It also has high technological applications when fabricated as a solid solution with PT as electrostrictive actuator and sensors. Hence the ML structure of PMN, the simplest among the distorted perovskite systems, and PT, a well-known FE, could be useful candidates for both fundamental understanding and for technological applications. Moreover, PMN has a good lattice matching with PT.

II. EXPERIMENTAL

Phase pure $Pb(Mg_{1/3}Nb_{2/3})O_3$ (PMN) and $PbTiO_3$ (PT) pellets were prepared through columbite process, and conventional solid state reaction process, respectively.[29] Well-sintered pellets of both PMN and PT were used as target materials for fabrication of thin films in a multitarget laser ablation chamber. Multilayer (ML) structures of PT and PMN were fabricated using a KrF pulsed excimer laser (Lambda Physik, 248 nm) fired at a pulsed energy of 120 mJ and a fluence of 3.5 J/cm^2. ML structures of different periodicities ranging from 10 to 70 nm in steps of 10 nm were fabricated on ⟨111⟩ oriented $Pt/TiO_2/SiO_2/Si$ substrates at 650 °C and 100 m Torr of oxygen ambient. All the ML structures were fabricated with a symmetric periodicity; hence, the PT and PMN were of equal thickness in a given period. A thin layer (50 nm) of $La_{0.5}Sr_{0.5}CoO_3$was used as a template layer to assist phase formation whose usage is well known in the fabrication of relaxor thin films.[30] The periodicity (d) and crystallinity of these structures were confirmed from the x-ray diffraction studies ($FeK_\alpha, \lambda = 1.936$ Å). The periodicities were compared with the thickness calibration done with respect to number of laser pulses using a cross sectional scanning electron microscope. The films grown under the processing conditions explained above were known to have a high orientation along (100) direction. The electric polarization and capacitance-voltage studies of these films were performed using an RT66A system working under modified Sawyer Tower circuit mode[31] and an impedance analyzer (4294A Agilent technologies).

III. RESULTS AND DISCUSSION

Figure 1 shows the x-ray diffraction (XRD) pattern of the ML and was found to be highly oriented along (100) direction. Figure 1(a) indicates the XRD pattern of a ML structure with a periodicity of 40 nm. Figure 1(b) shows the magnified view of the XRD pattern of the ML structures with different periodicity. The pattern clearly shows the presence of satellite reflections in the ML with the periodicities ranging from 20–50 nm which is a clear illustration of the superlattice type of behavior in the highly oriented polycrystalline structures for certain dimensions (20–50 nm). Periodicity of the superlattice structures was calculated from XRD pattern using the formula given below.[32]

$$d = \frac{\lambda}{2(\sin\theta_1 - \sin\theta_2)} \cdots . \quad (1)$$

θ_1 and θ_2 are the corresponding Bragg angles of the 1st and 2nd satellite reflections. The calculation from the XRD patterns matched well with the thickness calibration carried out on individual layers, bilayers, and ML for various number of laser pulses using a scanning electron microscope. Asymmetries present in the intensity distribution of the superlattice reflections have been studied extensively by static phonon approach and structure factor calculations[33] and are attributed to the fluctuation in the periodicity of the system. This could be due to the annealing effect experienced by the initial layers of deposition until the top layers are completed, which is unavoidable. Moreover, the second order term corresponding to the strain variation and the corresponding modification of structure factor introduces an asymmetry in the intensity distribution.[33] The satellite peaks were observed only for samples with a periodicity ranging between 20 and 50 nm. Samples with a periodicity of 10 nm show a broad single peak indicating a large strain present in the system. At 10 nm periodicity, the average $d_{(100)}$ was found to be $\sim$3.947 Å and the average $d_{(100)}$ spacing had a systematic decrease to 3.881 Å for 30 nm, and at 60 nm periodicity it

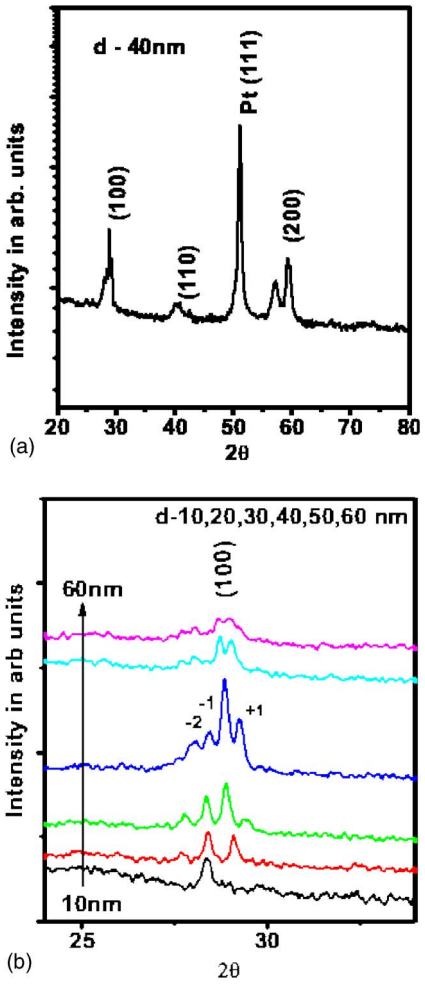

FIG. 1. (Color online) (a) XRD pattern of a highly oriented PT-PMN ML of 40 nm periodicity. (b) Magnified view of the (100) reflection of multilayers of all periodicities.

relaxed to 3.901 Å which matches very well with the bulk $d_{(100)}$(3.900 Å) of PT (74-2495, JCPDS-1999). On comparison with the bulk values of the $d_{(100)}$(4.044 Å) spacing of PMN (81-0861, JCPDS-1999) and PT, it is clear that the PT layers have undergone a tensile stress and the PMN a compressive stress.

The microstructural feature of a ML structure across the film is shown in Fig. 2. An oriented columnar growth of the ML with a column diameter of 30 nm and length of 600 nm was observed from a field emission scanning electron microscope (Sirion). Weak striations observed across the column of a single grain are due to the alternate layers of the ML present in a single column. This observation of a columnar growth of the whole structure indicates a sharp interface between the PT-PMN layers and also the absence of any grain boundary perpendicular to the applied field. Hence the influence of grain boundaries perpendicular to the applied electric field can be neglected in the present case and a single column of grain can be assumed as a single crystal of the ML structure.

Figure 3 shows the polarization behavior of the PT-PMN superlattice structures of different periodicities. The figure shows the presence of size dependent polarization behavior

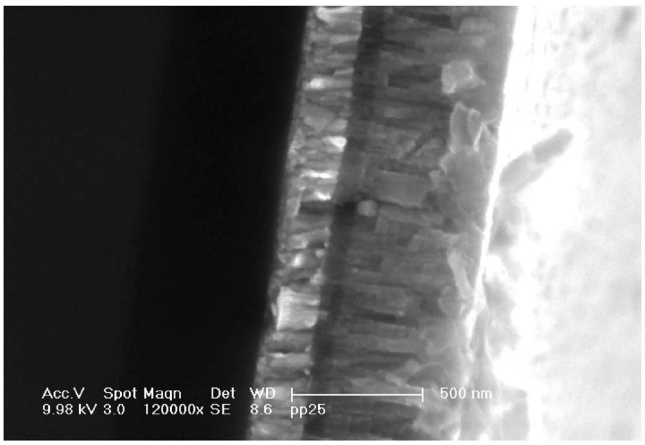

FIG. 2. Cross sectional SEM image of a PT-PMN ML with a periodicity of 50 nm.

of the ML. At a periodicity of 10 nm, the system exhibited a slim loop hysteresis similar to a solid solution of a PMN-PT relaxor material. On increasing the periodicity, they exhibited an antiferroelectric (AFE) type of behavior, showing a slim double hysteresis loop type of behavior normally observed for an AFE material. The existence of AFE coupling between the layers was observed in the periodicities of the range of 20–50 nm. On further increase of periodicity, a normal FE behavior was onset with a slim polarization loop characteristics.

The polarization behavior of any FE thin film structure is dominated by various intrinsic and extrinsic factors. The major factors that affect the polarization curves are (i) the FE domains and the dipolar interactions (short and long range), (ii) the depolarizing field, (iii) the electrode effects, and (iv) the other free charges due to defects, misfit dislocations etc., present in the system. In the case of heterostructures, the field generated at the interface due to the variation of polarization at the interface is another factor that could play a crucial role in stabilizing the ground state of the system. All the factors explained above have their own length scales over which they dominate.[11,19] The polarization behavior of the PT-PMN ML exhibited a size dependent interfacial coupling between the layers.

Existence of FE characteristics at a periodicity of 10 nm could be due to the domination of long-range interactions among the electric dipoles present. The existence of long-range interaction in a normal FE superlattice has been observed both theoretically and through experiments.[6,21,22] In the theoretical models, the Hamiltonian of the system is constructed based on a transverse Ising model (TIM).[6] The Hamiltonian constructed based on a TIM model involves coupling constants between the dipoles present at the interfaces of the two different FE layers A and B, and the coupling varies with distance as a power law as given below.[6]

$$J(r) \sim \frac{1}{r_{ij}^{\sigma}} \ \ldots , \tag{2}$$

where $J(r)$ is the exchange interaction and r_{ij} is the distance between two dipoles at sites i, j, and σ represents the decay-

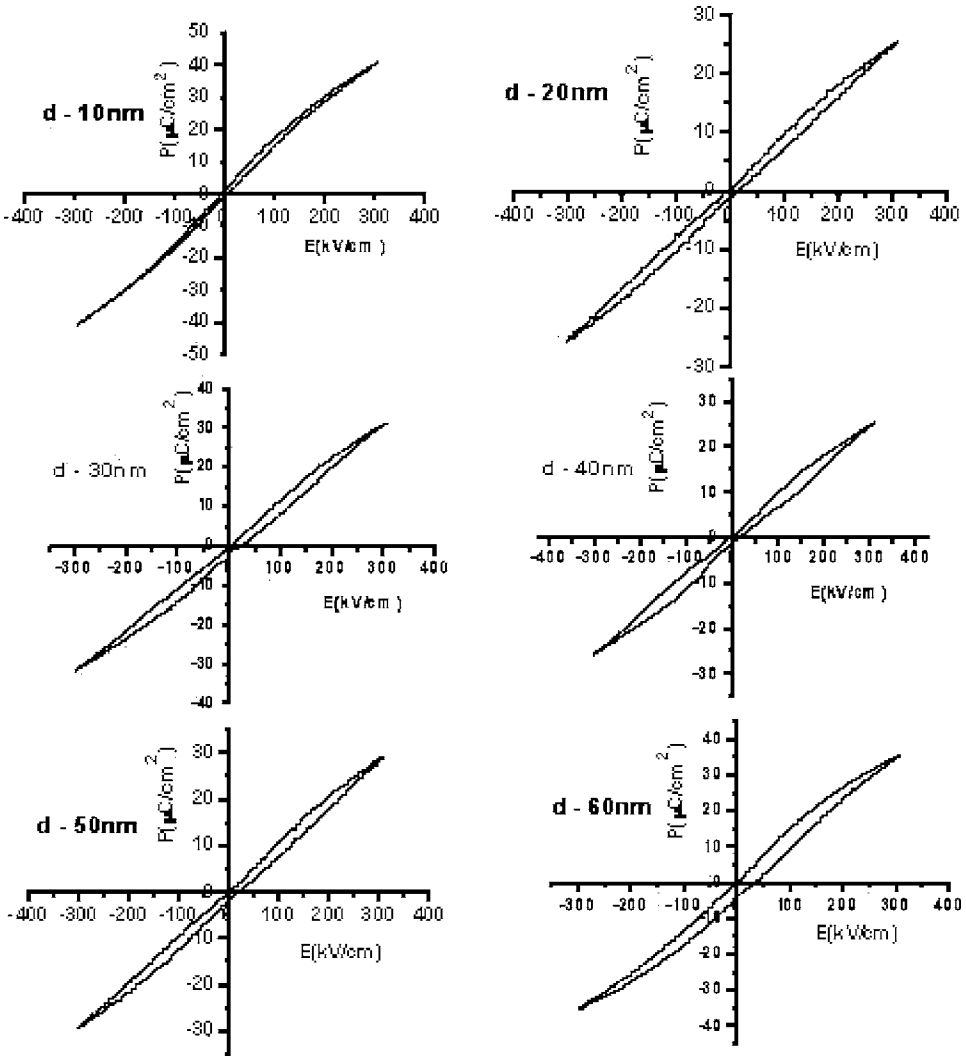

FIG. 3. Room temperature polarization hysteresis of the PT-PMN ML with different periodicity.

ing exponent. $J(r)$ transforms to interfacial coupling when the i^{th} dipole belongs to material A and the j^{th} dipole belongs to material B. At lower values of σ, the long-range interaction dominates and the heterostructure exhibits an averaged property of the existing materials. The existence of the long-range interaction was observed for about ~10 nm from the calculations,[6] which coincides with the experimental observations. Hence, the interfacial strain and the existence of long-range interaction between the adjacent layers of PT and PMN present in the ML could be responsible for the FE characteristic of the ML with 10 nm periodicity. The ML fabricated were highly oriented columnar structures and not epitaxially grown. At low periodicity of 10 nm, though the dimensions are within the range of the domination of long-range interaction of the dipoles, a collective effect of the interfacial roughness, the field at the interfaces due to polarization mismatch and the polarization of the system stabilizes the normal FE behavior and effectively exhibiting an averaged property of the constituent materials present in the ML structure. The slim loop FE type polarization behavior is insufficient to conclude the existence of long-range interaction in PT-PMN ML at 10 nm periodicity. A detailed crystal structure analysis on epitaxial ML is essential to prove and understand the FE distortions of PT and PMN and the dominance of long-range interactions between the two layers at low dimensions.[5]

On increase of periodicity, the dimensions of the individual layers exceed the critical size over which the polarization behavior of the PT-PMN ML is dominated by the interfacial coupling among the layers. The layers can be treated as a continuum and the interaction among the dipoles are overcome by the interfacial coupling and gives rise to an antiferroelectric interfacial coupling among the polarization of the layers constituting the ML structure. Several models have been reported in the literature for the validity of the continuum models in the case of FE heterostructures and are also treated as the continuum limit of the transverse Ising model.[14] The free energy expansion for a simple bilayer model is given below.[15]

$$F = \frac{A_1}{2\varepsilon_o}P_1^2L_1 + \frac{B_1}{4\varepsilon_o^2}P_1^4 - P_1EL_1 + \frac{A_2}{2\varepsilon_o}P_2^2L_2 + \frac{B_2}{4\varepsilon_o^2}P_2^4 - P_2EL_2 + JP_1P_2 \ \ldots, \tag{3}$$

where A_1, B_1, A_2, and B_2 are the Landau coefficients of corresponding layer 1 and layer 2; P_1 and P_2 are the polariza-

tion of the layers; and L_1, L_2 denotes the thickness of the individual materials. The last term is the interfacial coupling term, which governs the ground state of the system. J is the exchange interaction term between the layers at the interface.

The interfacial exchange interaction (J) between the polarizations of the two different layers present is treated as an analogue of the exchange interaction among the individual dipoles in the TIM.[6,7,19] The above equation, however, explains a FE heterostructure; it requires few corrections in terms of the role of depolarization field and the field due to the polarization mismatches at the interface, moreover the AFE coupling is assumed a priori and the dimensional dependence of the polarization behavior is calculated for unequal thicknesses of the individual layers. These corrections would play a crucial role in the calculation of the exact length scales over which the various extrinsic and intrinsic factors dominate. Hence the size dependence of the polarization hysteresis is less accurate in the case of the above-explained continuum model. The exchange interaction of the dipoles at the interface has to be taken into account in order to explain the multiple loop characteristics of a FE multilayer and a superlattice. The basic discrete TIM model, including the exchange interaction of the dipoles at the interface explaining the multiple loop behavior due to the effect of the intrinsic coupling and the interfacial coupling, consists of a Hamiltonian as given below.[19]

$$H = -\sum_{\langle i,j \rangle} J_{i,j} S_i S_j - \sum_i \Omega_i S_i^x - 2\mu E \sum_i S_i^z \ \ldots \qquad (4)$$

J_{ij} is the coupling constant among the dipoles present within a layer when the i^{th} dipole and j^{th} dipole belong to the same layer, and it turns out to be the interfacial coupling term when the i^{th} dipole and the j^{th} dipole belongs to the adjacent layers. S_i^x and S_i^z are the components of the spin operator in the case of magnetism and they mimic the dipole moment present in the FE systems. Ω_i is the transverse field across each layer and the third term couples the system with the applied electric field. The positive values of J favor FE coupling and negative values of J favor AFE coupling in terms of minimization of the free energy. The existence of the competition between the interfacial coupling and the applied field gives rise to a multiple loop behavior such as a conventional AFE system. A similar behavior was observed in the polarization hysteresis of the PT-PMN multilayers in a dimensional range of 20–50 nm of periodicity. At low fields there is a competition between the exchange interaction among the dipoles and the applied field, in which the exchange interaction dominates and effectively gives rise to an antipolar distortion at the PT-PMN interface. Hence a very low polarization at low applied fields is observed. At higher applied fields the applied field dominates over the AFE exchange interaction and results in a coherent rotation of all polarization domains parallel to the applied field. This behavior effectively gives rise to an AFE-like polarization behavior to the ML. On increase of the applied field, it overcomes the interfacial exchange interaction among the layers and results in the coherent rotation of all polarization domains parallel to the applied field and effectively exhibits FE characteristics. The observation of the double hysteresis behavior like a conventional AFE system is due to the antipolar alignment of the dipoles of PT and PMN at the interface, in order to minimize the energy of the system. In the above explained model,[19] the dimensional dependence of the polarization hysteresis has been explained by maintaining an unequal thickness among the given period. Hence, the model does not explain the dimensional dependence for equal reduction of individual layer thicknesses. The modification of the Hamiltonian to explain the whole ML stacking has been proposed by other authors.[6,7] But, those studies were concentrated over the phase transition behavior of the ML and not over the role of the interfacial coupling and the dimensional range over which it dominates the polarization behavior. The phase transition behavior is proved to be insensitive to the nature and strength of the interfacial coupling by those models[6,7] and the same has been observed later in this study. The interfacial coupling dominates the short- and long-range interactions in a dimensional range of 20–50 nm in the case of PT-PMN multilayers. Dimensional range over which the AFE coupling dominates the polarization and the strength of the coupling is further analyzed.

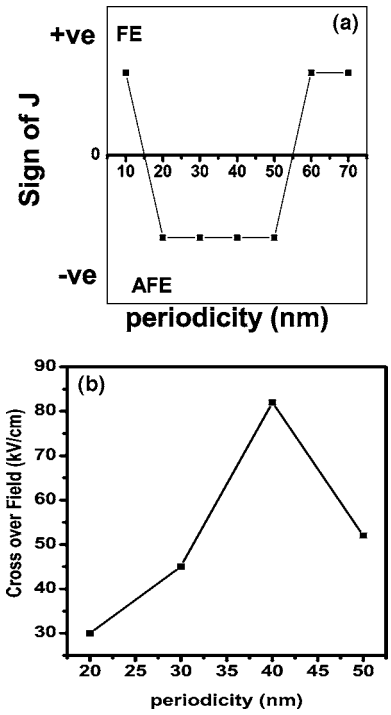

FIG. 4. (a) The variation of the sign of interfacial coupling (J) among the layers with periodicity. (b) The variation of the AFE to FE crossover field with periodicity.

Figure 4(a) shows the variation in the sign of J the interfacial exchange interaction with size as observed in the PT-PMN multilayers. Size dependence of the AFE to FE crossover field within the dimensional range of 20–50 nm is shown in Fig. 4(b). On increase of periodicity from 20 to 40 nm, the crossover field was found to increase from 30 kV/cm to 82 kV/cm, and on further increase of periodicity to 50 nm it again decreases to 52 kV/cm. The above observation of the increase of the crossover field on increase of periodicity could be due to the competition between the interfacial interaction (J) and the long-range ferroelectric in-

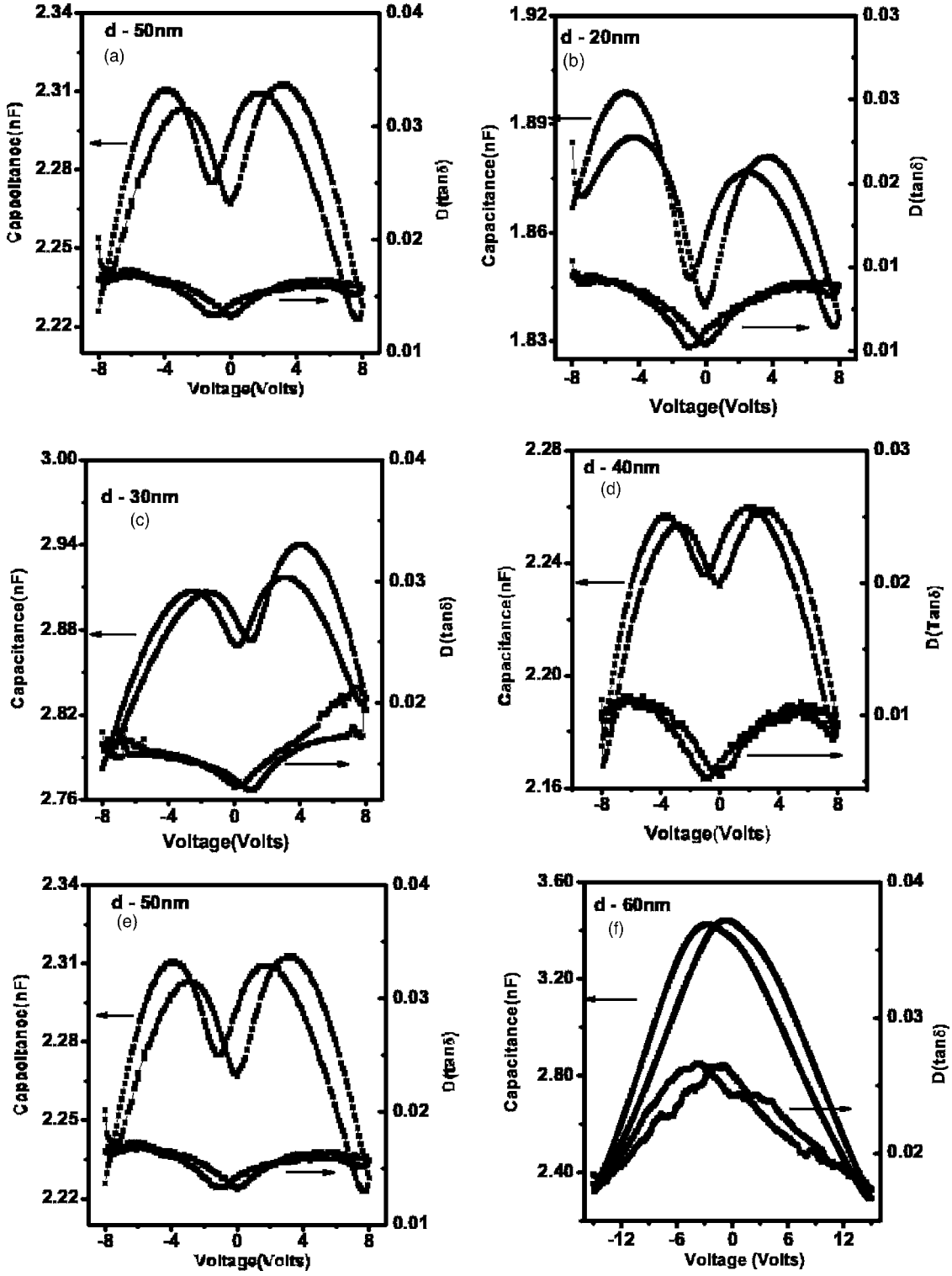

FIG. 5. Capacitance-voltage characteristics of the PT-PMN ML with varying periodicity [(a–f)-(10–60 nm) respectively].

teractions. At 20 nm, the interfacial coupling is weak and it gradually dominates over the long-range interaction on increase of periodicity, and hence the interfacial interaction is strong at 40 nm periodicity. On further increase of periodicity the J is again dominated by the intrinsic short-range FE interactions present in the system and again a drop in the strength of the interfacial coupling is observed at 50 nm. On increase of periodicities to 60 nm and above, only FE behavior was observed. In this regime the dimensions of the individual layers of the ML are beyond the length scale over which the intense interfacial couplings or the long-range interaction among the layers could dominate the property of the ML structure. The intrinsic short-range dipolar interactions dominate and the system exhibits the bulk characteris-

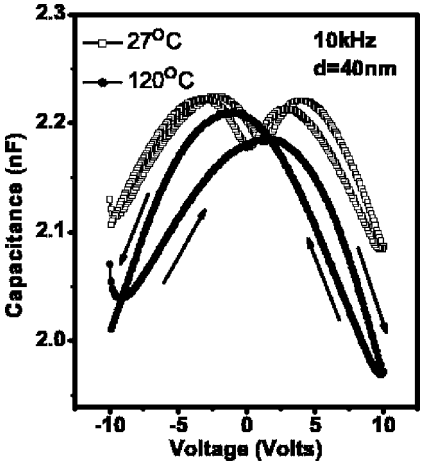

FIG. 6. Temperature dependent variation of C-V curve exhibiting AFE and FE behavior at low and high temperatures, respectively, for a PT-PMN ML with periodicity of 40 nm.

tics of the individual material as two FE put together.[6,7] The domination of interfacial coupling over the short- and long-range interactions stabilizes the AFE behavior in the observed dimensional range. Effectively the AFE behavior observed in a range of periodicity of these ML is due to the externally induced heterogeneous polarization and not an intrinsic property normally observed as antidipolar distortions in individual materials such as $PbZrO_3$.[34]

To further confirm the indication from the FE slim loops and the AFE behavior the capacitance-voltage (CV) measurements were carried out on these samples to cross check the polarization behavior. The CV curves may not be exactly the slope of the P-E curves due to their difference in the measurement techniques; however, this could be a useful experiment to mimic the slope of the P-E curves and a useful approach to confirm the polarization behavior.[35] Figure 5(a)–5(f) shows the room temperature CV characteristics of the PT-PMN superlattices of different periodicities measured at 10 kHz. The results indicate clear size dependence exactly similar to the corresponding conventional polarization curves. A butterfly loop CV behavior is a common phenomenon observed in normal FE compositions.[26] A butterfly loop with a valley at the zero bias is a well-known illustration of an antiferroelectric behavior.[26] The factors that dominate the P-E curves also influence the CV characteristics in the similar fashion. Hence, from the observed P-E and CV curves, a clear size dependent characteristic is evident and their interfacial interaction follows the trend as shown in Fig. 4.

The role of the interfacial interaction on stabilizing the AFE behavior is further envisaged through the studies of the temperature variation of the CV and P-E characteristics. PMN is known to have a transition from a FE to PE phase below room temperature, as explained earlier.[26] But the existence of the remnant polarization well above the transition temperature is a common phenomenon observed in relaxor ferroelectrics.[25] To understand and confirm the role of interfacial interaction in exhibiting an AFE behavior, the polarization studies were repeated at temperatures well above the T_m of PMN. At temperatures above T_m, PMN transforms to a PE state, effectively transforming a FE-FE interaction to a

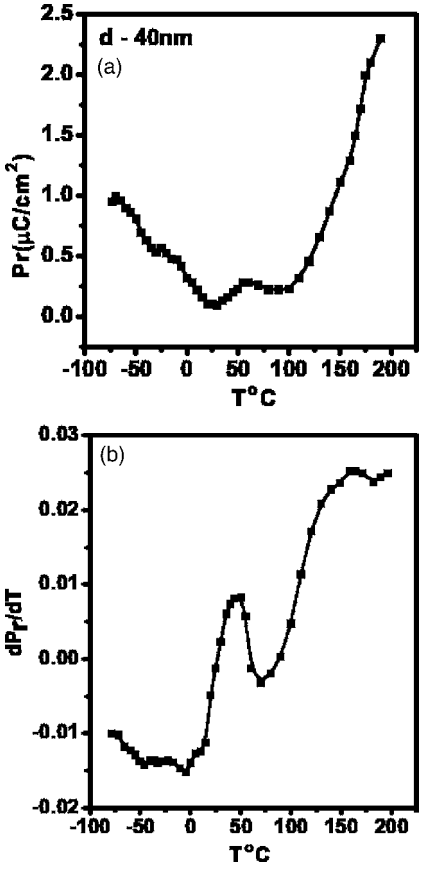

FIG. 7. (a) Variation of remnant polarization (P_r) with temperature of a PT-PMN ML with a periodicity of 40 nm. (b) Variation of dP_r/dT with temperature for a PT-PMN ML with a periodicity of 40 nm.

FE-PE interaction and hence, the AFE behavior is expected to diminish at temperatures well above T_m. Both PE and CV measurements were carried out in the temperature range of −70 to 180 °C. The AFE behavior was observed until 70 °C and above which only normal FE behavior was observed. The CV curves at two different temperatures are shown in Fig. 6. At temperatures above 50 °C, the interlayer interaction becomes a FE-PE interaction rather than a FE-FE interaction, hence, effectively indicating the ferroelectric behavior of the PT layer. An AFE behavior was observed on cooling back to room temperature, which indicates the reversible transformation of the interfacial interaction. Polarization curves were measured at various temperatures and their remnant polarization (P_r) was found to be very low until 50 °C due to their AFE coupling, and above that they exhibited a normal FE loop characteristic with enhanced P_r. Figure 7(a) and 7(b) show the variation of Pr and dP_r/dT with temperature. The dielectric dissipation factor (tan δ) of the system was 0.014 and 0.023 at room temperature and 180 °C, respectively. Hence, the high temperature measurements of the polarization curves are the actual polarization loops and were not interfered with by the leakage current of the system.[22] The hump in the dP_r/dT at 50 °C can be used as a point where the FE-FE interfacial interaction breaks up and the system goes to the effective FE character due to the FE behavior of the PT layers.

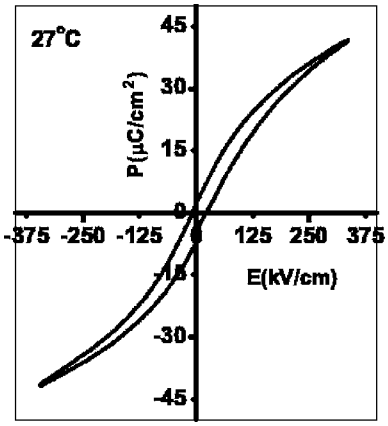

FIG. 8. Room temperature polarization behavior of a PMN thin film.

The variation of P_r with temperature and the variation of dP_r/dT with temperature for a ML structure with a periodicity of 40 nm clearly show that the AFE behavior is an interface-dominated phenomenon.[22] The AFE to FE transition at 50°C is clearly due to the transformation in the interfacial interaction present between the layers. The reversible nature of the interfacial coupling confirms the possibility of the local transition among the PMN layers and the presence of PT plays a role in shifting the transition of PMN to higher temperature. Thus the temperature variation on the PE and CV studies of these multilayers proves that the observed AFE response is strongly due to the interfacial coupling present in the ML structures, which is an extrinsic effect and not an intrinsic antipolar distortion among the dipoles within a single layer, as observed in homogeneous single layer AFE thin films such as $PbZrO_3$.[34] An AFE-like double loop behavior has also been observed in a homogenous defect induced FE,[28] and a disordered bulk relaxor FE above the transition temperature due to the presence of defects introduced due to various processing conditions.[36] The possibility of the appearance of double loop hysteresis due to the defects in the case of PMN layers was studied further. The concentration of oxygen vacancies are known to be tunable with variation of processing conditions,[36] in our case mainly the oxygen ambient and the growth temperature. Hence, polarization studies of the homogeneous PMN layers fabricated at the same process conditions were carried out at different temperatures. There was no sign of AFE-like behavior at any of the measured temperatures (−70 to 50°C) and the room temperature polarization loop of a homogeneous PMN layer is shown in Fig. 8. Hence the observed double loop behavior is not due to an antipolar distortion due to the presence of a high concentration of oxygen defects in the relaxor FE at temperatures above T_m.[36] Though the existence of thermodynamically stable oxygen defects at low concentration is unavoidable, those defects are not responsible for the appearance of a double loop in the polarization behavior of the PT-PMN ML.

The polarization behavior of the PT-PMN ML exhibited a clear size dependent FE and AFE behavior. The AFE coupling could be understood from the energy arguments based on the competition between the interfacial coupling and the

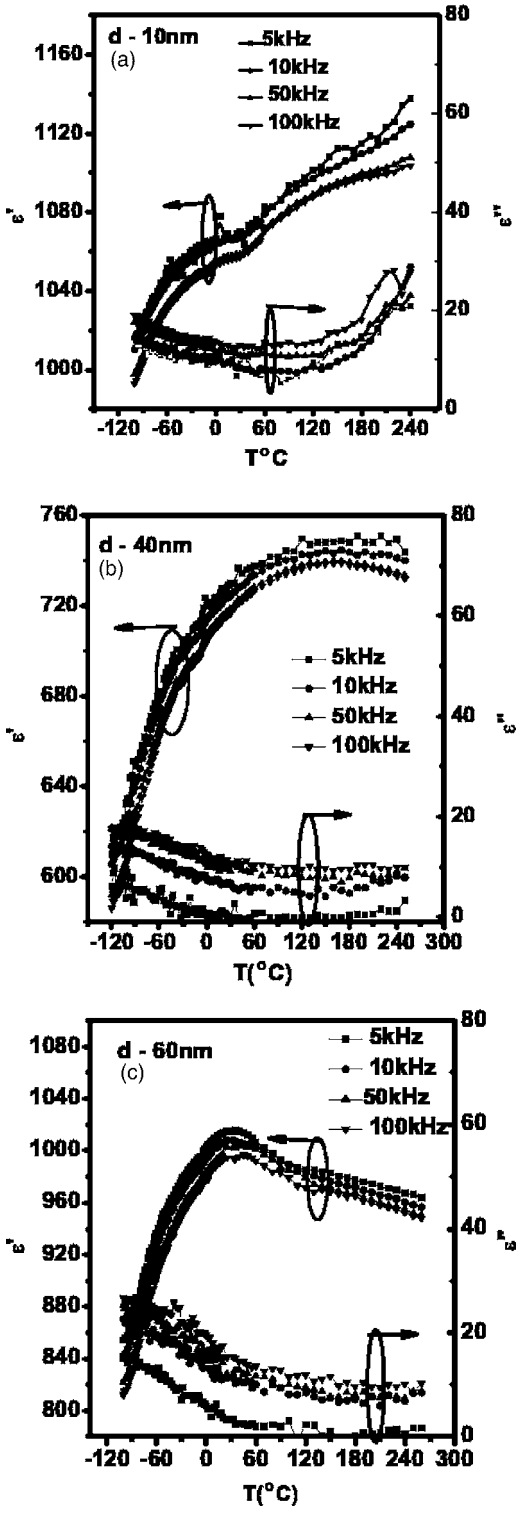

FIG. 9. Dielectric phase transition behavior of the PT-PMN ML with different periodicity [(a)–10 nm, (b) –40 nm, (c)–60 nm].

applied field. Existence of an averaged property at low periodicities and the behavior of individual materials at larger periodicities were further analyzed. The existence of an averaged physical property due to the presence of strain and long-range interaction at low periodicity (~10 nm) and the behavior of individual materials property at higher periodici-

ties (>60 nm) was further confirmed from the dielectric phase transition behavior of the PT-PMN ML structures. Figure 9 shows the dielectric phase transition of the PT-PMN ML structures with different periodicities. At low periodicity [Fig. 9(a)] of 10 nm, the ε' increases monotonously with increase of temperature (up to 250 °C) except a small drop in ε' at around 60 °C, which requires detailed studies before concluding as a transition. In general, the sample with 10 nm periodicity did not exhibit any feature of a relaxor in the phase transition studies, characteristic to a homogeneous single PMN layer within the measured temperature regime.[25,26] The measurements were not carried out beyond 250 °C due to the problems of gold diffusion and interference of space charge and DC leakage over the dielectric constant. Characteristic relaxor behaviors like frequency dependent T_{max} (temperature corresponding to thedielectric maxima) and the frequency independent behavior beyond the T_{max} were absent. ML with periodicity ranging from 20–50 nm, where the AFE interfacial coupling dominated the polarization behavior of the system, exhibited a similar temperature dependent behavior irrespective of their periodicities. The dielectric phase transition behavior of a ML with 40 nm periodicity is shown in Fig. 9(b). Beyond the transition range of PMN single layers, the dielectric constant remained almost constant over a temperature range of −30 to 250 °C for all the ML with periodicity ranging from 20–50 nm, which could be a very useful feature for device applications. At higher periodicities, any FE heterostructure is generally expected to behave as individual materials put together, where the presence of one type of material A does not affect the characteristic feature of the other type of material B. Hence, for a periodicity of 60 nm, characteristics of individual PMN layers are expected to show up in the overall phase transition behavior of the ML structures. The phase transition studies of ML with 60 nm periodicity clearly exhibited a distinguishable characteristic feature of the individual materials constituting the ML structure. A clear normal relaxorlike behavior was observed at the temperature range as observed in the homogeneous single layers of PMN. This clearly indicates that at larger periodicities the ML structures behave as individual materials put together and no characteristics interlayer interaction is observed. The imaginary part of dielectric constant ε'' of MLs was very low, indicating a low dissipation of the materials under study. They exhibited almost similar behavior for all the ML with increase of temperature. The low values of the imaginary part of the dielectric constant indicates that the high temperature measurements are not interfered with by the other extrinsic effects such as space charge and DC leakage of the MLs. The dielectric phase transition behavior provesan average behavior at low periodicity of ~10 nm, and a temperature independent behavior in the range of −30 to 250 °C for the ML with periodicities in the range of 20–50 nm. The AFE interfacial coupling and the strength of the interfacial coupling are insensitive over the dielectric phase transition of the ML structures. At larger periodicity (~60 nm), the heterostructure exhibited a behavior of individual materials constituting the ML and was insensitive to the long-range interactions, interfacial coupling among the layers and they are purely dominated by the short-range intrinsic coupling of the individual materials, which is clear from their phase transition behavior.

IV. CONCLUSIONS

In summary, ML structures of different periodicities were fabricated through pulsed laser ablation technique; their interfacial coupling and their size dependence over the polarization behavior were studied. MLs with a periodicity of 10 nm exhibited a clear FE characteristic, similar to that of a solid solution, which is due to the dominance of the long-range coupling among the dipoles and the lattice strain present at the interface. On increase of periodicity from 20–50 nm, they exhibited an AFE behavior. Such behavior could be understood, based on the interfacial coupling among the layers present and energy arguments. The interfacial coupling gives rise to an AFE coupling which could be transformed to a FE coupling at larger applied electric fields, as observed in normal intrinsic AFE systems. Strength of the interfacial coupling was found to be high at 40 nm periodicity. Further increase of periodicity to 60 nm and above the system showed an average FE behavior, where again the short-range interaction of dipoles dominates the interfacial coupling and whole system behaves as two FE systems put together. The FE-FE layer interaction which stabilized AFE behavior at room temperatures transforms to a FE-PE layer interaction, hence exhibiting FE behavior at temperatures above the T_c of PMN. The temperature variation of P_r and dP_r/dT clearly establishes the transition between AFE to FE behavior with temperature, which is due to the variation of the exchange interaction of the individual layers at the interface. The existence of AFE behavior in the PT-PMN superlattices are purely due to the interfacial coupling which is an extrinsic effect and not an intrinsic behavior of the system as observed in conventional AFE systems. The presence of an averaged behavior at low periodicity and the behavior of individual materials put together at larger periodicity is further envisaged through phase transition studies. At intermediate periodicities (20–50 nm) the dielectric phase transition studies were insensitive to the AFE interfacial interaction among the layers, which was observed in the polarization studies. Nevertheless, the role of misfit dislocations and point defects at the interfaces over the interfacial interaction remains ambiguous; moreover, the existence and dynamics of the polar clusters of PMN at nanodimensions are under study.

*Authors to whom correspondence should be addressed. Electronic addresss: ranjith@mrc.iisc.ernet.in; sbk@mrc.iisc.ernet.in

[1] G. Rijnders and Dave H. A. Blank, Nature (London) **433**, 369 (2005).
[2] J. B. Neaton and K. M. Rabe, Appl. Phys. Lett. **82**, 1586 (2003).
[3] I. K. Schuller, Phys. Rev. Lett. **44**, 1597 (1980).
[4] D. P. Norton, B. C. Chakoumakos, J. D. Budai, D. H. Lowndes, B. C. Sales, J. R. Thomson, and D. K. Christen, Science **265**, 2074 (1994).
[5] J. M. Gregg, J. Phys.: Condens. Matter **15**, 11 (2003).
[6] J. Shen and Y. Q. Ma, Phys. Rev. B **61**, 14279 (2000).
[7] B. D. Qu, W. L. Zhong, and R. H. Prince, Phys. Rev. B **55**, 11218 (1997).
[8] C. Bungaro and K. M. Rabe, Phys. Rev. B **69**, 184101 (2004).
[9] J. B. Neaton and K. M. Rabe, Appl. Phys. Lett. **82**, 1586 (2003).
[10] Y. Q. Ma, J. Shen, and X. L. Xu, Solid State Commun. **114**, 461 (2000).
[11] V. A. Stephanovich, I. A. Lukyanchuk, and M. G. Karkut, Phys. Rev. Lett. **94**, 047601 (2005).
[12] C. Wang and D. R. Tilley, Solid State Commun. **118**, 333 (2001).
[13] B. Qu, W. Zhong, and P. Zhong, Jpn. J. Appl. Phys., Part 1 **84**, 4115 (1995).
[14] Y. Q. Ma, J. Shen, and X. H. Xu, Solid State Commun. **114**, 461 (2000).
[15] K. H. Chow, L. H. Ong, J. Osman, and D. R. Tilley, Appl. Phys. Lett. **77**, 2755 (2000).
[16] F. LeMarrec, R. Farhi, M. El. Marssi, J. L. Dellis, M. G. Karkut, and D. Ariosa, Phys. Rev. B **61**, R6447 (2000).
[17] J. C. Jiang, X. Q. Pan, W. Tian, C. D. Theis, and D. G. Schlom, Appl. Phys. Lett. **74**, 2851 (1999).
[18] X. S. Wang, C. L. Wang, and W. L. Zhong, Solid State Commun. **122**, 311 (2002).
[19] Y. Z. Wu, P. L. Yu, and Z. Y. Li, J. Appl. Phys. **91**, 1482 (2002).
[20] M. Sepliarsky, S. R. Phillpot, D. Wolf, M. G. Stachiotti, and R. L. Migoni, Phys. Rev. B **64**, 060101(R) (2001).
[21] E. D. Specht, H. M. Christen, D. P. Norton, and L. A. Boatner, Phys. Rev. Lett. **80**, 4317 (1998).
[22] M. H. Corbett, R. M. Bowmann, J. M. Gregg, and D. T. Foord, Appl. Phys. Lett. **79**, 815 (2001).
[23] H. M. Christen, E. D. Specht, S. S. Silliman, and K. S. Harshavardhan, Phys. Rev. B **68**, 020101 (2003).
[24] J. Sigman, D. P. Norton, H. M. Christen, P. H. Fleming, and L. A. Boatner, Phys. Rev. Lett. **88**, 097601 (2002).
[25] L. E. Cross, Ferroelectrics **76**, 241 (1987).
[26] D. Viehland, S. Jang, L. E. Gross, and M. Wuttig, J. Appl. Phys. **68**, 2916 (1990).
[27] D. Viehland, S. Jang, L. E. Gross, and M. Wuttig, Philos. Mag. B **64**, 335 (1991).
[28] M. E. Lines and A. M. Glass, *Principles and Applications of Ferroelectrics and Related Materials* (Clarendon Press, Oxford, 1979).
[29] S. Swartz and T. Shrout, Mater. Res. Bull. **17**, 1245 (1982).
[30] Apurba Laha, S. Saha, and S. B. Krupanidhi, Thin Solid Films **424**, 274 (2003).
[31] C. B. Sawyer and C. H. Tower, Phys. Rev. **35**, 269 (1930).
[32] F. Le. Marree, R. Farhi, B. Diehil, J. Chevreul, and M. G. Karkut, J. Eur. Ceram. Soc. **21**, 1615 (2001).
[33] Armin Segmiller and A. E. Blakeslee, J. Appl. Crystallogr. **6**, 19 (1973).
[34] S. S. N. Bharadwaja, P. Victor, P. Venkateswarulu, and S. B. Krupanidhi, Phys. Rev. B **65**, 174106 (2002).
[35] M. Dawber, K. M. Rabe, and J. F. Scott, Rev. Mod. Phys. **77**, 1083 (2005).
[36] F. Chu, N. Setter, and A. K. Taganstev, J. Appl. Phys. **74**, 5129 (1993).